

# Roaming in restricted acetaldehyde: a phase space perspective

Vladimír Krajňák, Stephen Wiggins  
*School of Mathematics, University of Bristol, UK*

Recent experimental and theoretical results show many molecules dissociate in a slow and complicated manner called roaming, that is due to a mechanism independent of the mechanisms for molecular and radical dissociation. While in most molecules the conventional molecular mechanism dominates roaming, acetaldehyde stands out by predominantly dissociating to products characteristic for roaming. This work contributes to the discussion of the prominence of roaming in (restricted) acetaldehyde from a dynamical systems perspective. We find two mechanisms consisting of invariant phase space structures that may lead to identical molecular products. One of them is a slow passage via the flat region that fits the term frustrated dissociation used to describe roaming and is similar to the roaming mechanism in formaldehyde. The other mechanism is fast and avoids the flat region altogether. Trajectory simulations show that the fast mechanism is significantly more likely than roaming.

## Introduction

Anomalies in experimental data for the photodissociation of formaldehyde,  $\text{H}_2\text{CO}$ , [1] have led to new understanding of the dissociation dynamics of formaldehyde [2–7] which has been referred to as the *roaming mechanism* for reaction dynamics. The widespread interest in this new reaction mechanism resulted in its discovery in a variety of reactions. Much of this work was described in the abundance of review papers that subsequently appeared [8–14].

This begs the question, “what is roaming”? In [15] it was noted that a dissociating molecule should possess two essential characteristics in order to label the reaction as “roaming”. In particular, the molecule should have competing dissociation channels, such as dissociation to molecular and radical products, and there should exist a long range attraction between fragments of the molecule. In a recent review article [14] Suits refines this definition of roaming even further by stating that “A roaming reaction is one that yields products via reorientational motion in the long-range ( $3 - 8\text{\AA}$ ) region of the potential”.

Following the seminal studies on roaming in the dissociation formaldehyde attention was focused on roaming in acetaldehyde,  $\text{CH}_3\text{CHO}$  [16–22]. Formaldehyde and acetaldehyde roaming dynamics present interesting contrasts. In formaldehyde the long range reorientational motion occurs between the  $\text{HCO}$  fragment and a hydrogen atom. In acetaldehyde the long range reorientation dynamics occurs between the  $\text{HCO}$  fragment and a methyl group,  $\text{CH}_3$ . Both molecules possess competing dissociation channels to molecular and radical products, with the molecular channel be identified with the roaming mechanism. However, it was found by trajectory analyses that for formaldehyde dissociation by roaming occurred much less frequently than dissociation to radical products and but that the opposite occurred for acetaldehyde. A reason for this could be the mass difference in the roaming fragment; H for formaldehyde and  $\text{CH}_3$  for acetaldehyde.

The question of the mass dependence of the roaming mechanism was investigated in [23] using a model that has been shown to exhibit the essential features of roaming, the Chesnavich model [24] for the reaction  $\text{CH}_4^+ \rightarrow \text{CH}_3^+ + \text{H}$  [15, 25, 26]. An advantage of the Chesnavich model is that it is analytical and therefore the parameters that describe the reaction can be varied. In particular, the mass of the roaming fragment, H can be varied and we can study the effect of this variation on the roaming mechanism to dissociation. Following a detailed analysis of trajectories and the structures in phase space responsible for roaming, it was found that the variation of the mass of the roaming fragment had no significant effect on the quantity of trajectories dissociating via the roaming channel.

This seemed to be somewhat at odds with the formaldehyde/acetaldehyde results on the importance of roaming for dissociation. Perhaps the discrepancy could be attributed to the simplicity of the Chesnavich model in comparison to the formaldehyde and acetaldehyde models. However, recently work [27] raises questions about the nature and quantity of trajectories undergoing dissociation of acetaldehyde due to roaming.

In this paper we pursue this question using a phase space approach for revealing the roaming mechanism that was previously carried out for formaldehyde [28]. In that work it was shown that the phase space setting allowed one to determine whether or not a specific trajectory dissociated to molecular or radical products. In particular, it was shown that the stable and unstable manifolds of certain periodic orbits defined an energy surface landscape that governed whether or not a trajectory dissociated to molecular or radical products. Due to the unboundedness of the energy surface that is characteristic for all dissociation problems, the ergodic hypothesis fails for roaming systems and invalidates standard statistical methods for reaction dynamics.

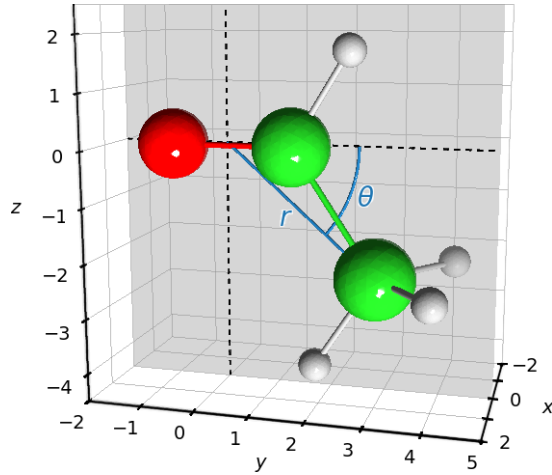


FIG. 1. Illustration of polar coordinates describing the position of the centre of mass of  $\text{CH}_3$  on the HCO plane given by  $x = 0$ .

In this paper we carry out a similar phase space analysis for a restricted acetaldehyde. Our results indicate that the dissociation dynamics of acetaldehyde is very similar to that of formaldehyde. In particular, the relative number of trajectories that dissociate to molecular or radical products is similar for both molecules. This is consistent with the results in [23]. Furthermore we find a mechanism that is much faster and avoids “reorientational motion in the long-range region of the potential”, yet may lead to the same molecular products as roaming. This agrees with the findings of [27] and deserves further attention.

### System

Derived from a potential for acetaldehyde used in [29] and based on [18] kindly provided by Prof. J. Bowman, Prof. Y.-C. Han and Prof. B. Fu, we study a restricted Hamiltonian system with 2 degrees of freedom. Our system assumes HCO and  $\text{CH}_3$  to be rigid bodies with configurations given by the minimum potential energy in the acetaldehyde well. Moreover, the centre of mass of  $\text{CH}_3$  moves in a centre of mass frame on the plane defined by HCO. The orientation of  $\text{CH}_3$  is fixed so that all internal angles as well as angles with respect to the position vector of the centre of mass of  $\text{CH}_3$  remain constant. In this configuration  $\text{CH}_3$  is always facing HCO carbon first.

Our system is defined by the Hamiltonian

$$H(r, \theta, p_r, p_\theta) = \frac{p_r^2}{2\mu} + \frac{p_\theta^2}{2} \left( \frac{1}{I_{\text{HCO}}} + \frac{1}{\mu r^2} \right) + U(r, \theta), \quad (1)$$

where  $r, \theta$  are the polar coordinates of the centre of mass of  $\text{CH}_3$  on the plane defined by HCO in atomic units and radians respectively (Fig. 1),  $p_r, p_\theta$  are the momenta canonically conjugate to  $r, \theta$  respectively,  $\mu = 18040.89 m_e$  is the reduced mass of  $\text{CH}_3$ ,  $I_{\text{HCO}} = 81448.95123 m_e a_0^2$  is the moment of inertia of HCO and  $U$  is the potential energy in hartree derived from the acetaldehyde potential as described above. We investigate the system at a fixed total energy  $H = 0.01$  a.u. above the dissociation threshold  $E_d = -153.440526848047$  a.u.

A contour plot of  $U$  in cartesian coordinates is shown in Fig. 2. Critical points, their coordinates and energies (with respect to  $E_d$ ) are listed in Tab. I and displayed in Fig. 3.

There are three potential wells near HCO, the deepest of which is the acetaldehyde well near C (further referred to as the C-well). The well near H (H-well) is relevant to roaming, as this is where in the full system  $\text{CH}_3$  abstracts H from HCO. These wells are separated by an index-1 saddle and an index-2 saddle. Both wells are connected to the flat region via index-1 saddles with energies below the dissociation threshold. A third potential well near O is inaccessible at  $H = 0.01$  a.u.

Trajectory simulations suggest the presence of two different mechanisms responsible for transport between the C-well and the H-well - a fast mechanism and a slow mechanism. Fig. 4 shows the escape/capture times of 767266 trajectories leaving the C-well initialised uniformly on the appropriate dividing surface defined in the Supporting information. Of those 627506 dissociated, 1522 entered the C-well, 138238 entered the H-well - but only 1221 took

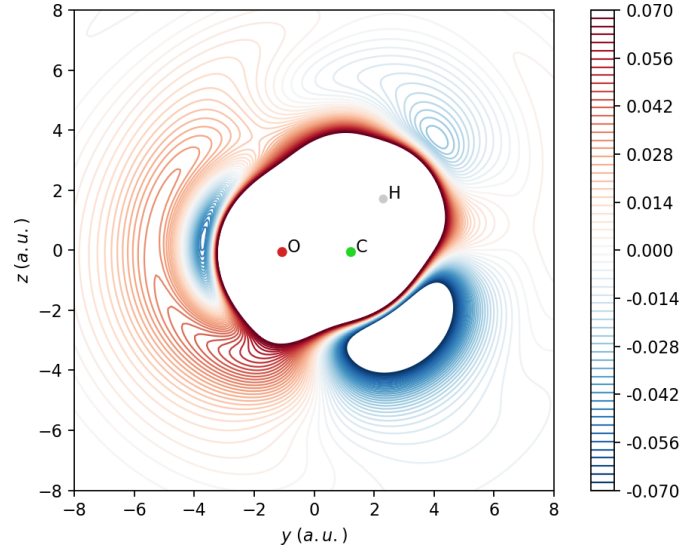


FIG. 2. Contour plot of the potential energy surface showing potential wells (blue) and areas of high potential (red).

Energy (hartree)	$r$ (a.u.)	$\theta$ (radians)	Significance	Label in Fig.
-0.16116	3.85430	-0.72053	C-well (acetaldehyde)	●
-0.02910	5.55601	0.73850	H-well	●
0.00300	6.93530	0.12084	saddle between C-well and H-well	×
0.00188	8.77285	1.26013	saddle between H-well and flat region	×
0.00616	8.75635	0.19413	index-2 saddle	▲
-0.00381	10.30339	2.01440	well in the flat region	●
-0.00246	10.29796	-1.87346	saddle in the flat region	×
-0.00233	11.50929	-0.07327	saddle in the flat region	×
-0.05092	3.71536	3.03771	O-well	●
0.01752	4.16820	2.05342	saddle between H-well and O-well	×

TABLE I. Critical points of the potential  $U(r, \theta)$ . Positions are shown in Fig. 3

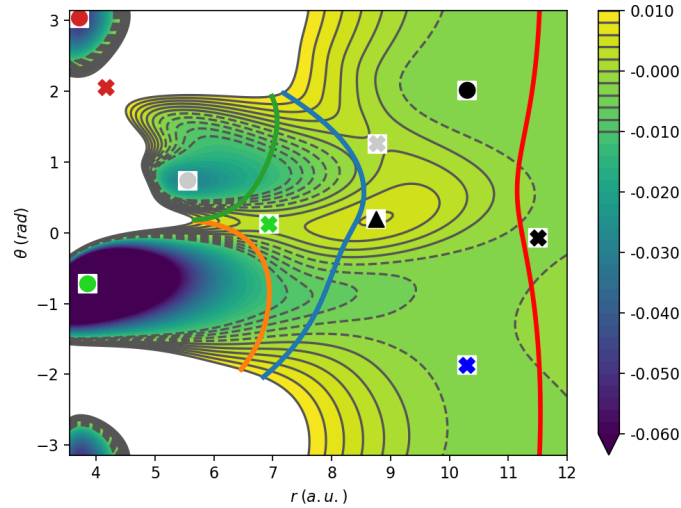


FIG. 3. Configuration space projections of relevant periodic orbits, with the outer periodic orbits ( $r \approx 22.9$ ) left out for the sake of readability. Critical points of the potential are shown and listed in Tab. I. Local minima are marked with a circle, index-1 saddles with a cross and an index-2 saddle with a triangle.

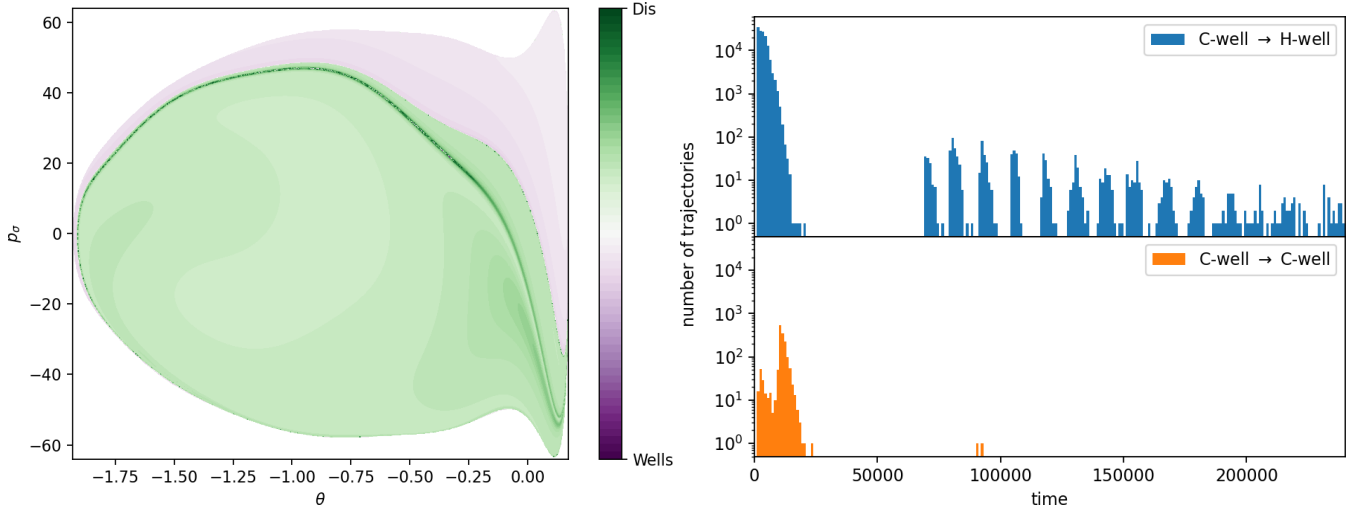


FIG. 4. Escape/capture times of trajectories leaving the C-well initialised uniformly on the outward half of  $DS_C$  for  $H = 0.01$ . Left: Initial conditions that lead to radical dissociation are shown in shades of green, trajectories that enter either of the wells in purple. Dark shades indicate long escape/capture time, light shades short.  $p_\sigma$  on the vertical axis is the momentum canonically conjugate to  $\theta$  on  $DS_C$ . Right: Histograms of capture times of the corresponding trajectories terminated in the H-well and the C-well respectively. The vertical axis is in log scale.

longer than 50000 time units, see Fig. 4. We explain how stable and unstable invariant manifolds of unstable periodic orbits convey trajectories between the two wells in phase space.

### Relevant periodic orbits

We identified several vibrational and rotational periodic orbits that govern the dynamics of the restricted acetaldehyde, the configuration space projection of four of which are shown in Fig. 3. Note that rotational periodic orbits always come in pairs with identical configuration space projection and opposite orientation - one rotating clockwise and one counter-clockwise. Most of these orbits and their dynamical significance are similar to those found in other roaming systems such as formaldehyde [28], Chesnavich's  $CH_4^+$  system [15, 26] or the double Morse system [30]. These are

- a pair of nearly circular ( $r \approx 22.9$ ) unstable outer periodic orbits which marks the point of radical dissociation,
- an unstable orbit delimiting the C-well,
- an unstable orbit delimiting the H-well,
- a pair of periodic orbits in the flat region.

We refer to these orbits as the outer orbit(s), the C-orbit, the H-orbit and the f-orbit(s) respectively. The outer orbits are due to a centrifugal barrier [26].

The dividing surfaces  $DS_C$ ,  $DS_H$  and  $DS_f$  are defined as the surfaces on the  $H = 0.01$  energy surface that have the same configuration space projections as the C-orbit, the H-orbit and the f-orbit(s) respectively. This construction is due to [31, 32] and details are provided in the Supporting information.  $DS_C$  and  $DS_H$  delimit the analogue of the respective potential wells in phase space. We refrain from using the term 'transition state' due to its ambiguous use in the literature for both unstable periodic orbits and the associated dividing surfaces.

Unlike the system mentioned above, a crucial role in acetaldehyde is played by another orbit, referred to as the CH-orbit:

- an unstable periodic orbit that lies between the C- and H-wells and the flat region.

Unstable periodic orbits are located in phase space bottlenecks, thanks to which the corresponding DS has locally minimal flux [33, 34]. This bottleneck allows certain trajectories to pass, while preventing others from doing so. The selection is due to the stable and unstable invariant manifolds [35–37] of the unstable periodic orbit. This leads to two

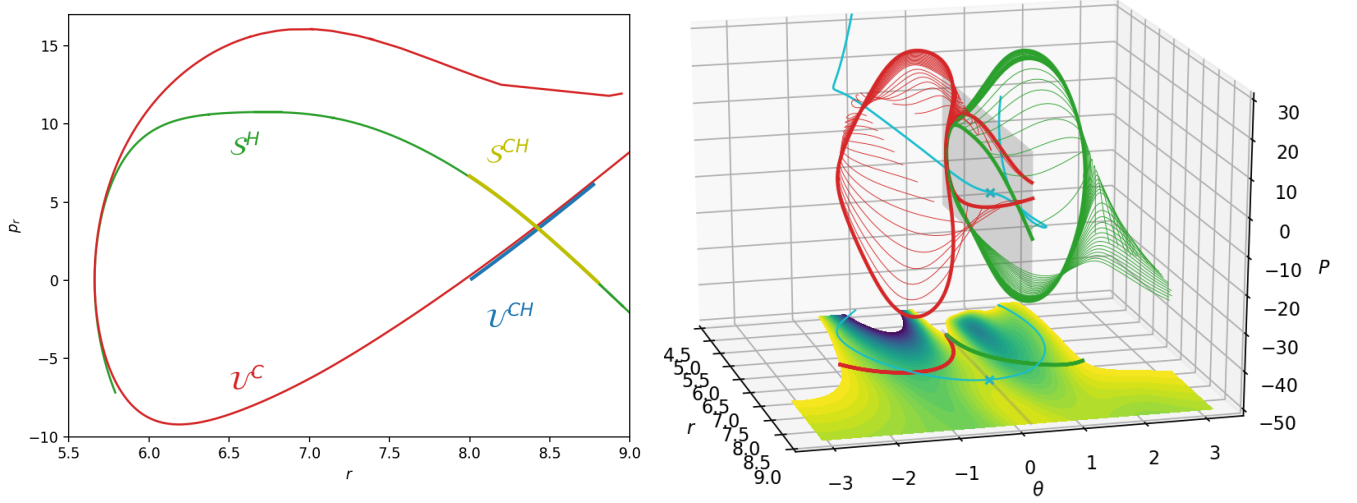


FIG. 5. The fast mechanism conveying trajectories from the C-well to the H-Well. Left: Intersection of  $\mathcal{U}^C$  and  $\mathcal{S}^H$  on  $\theta = 0.177$ ,  $p_\theta > 0$ . Right: A 3-dimensional representation of the intersection of  $\mathcal{U}^C$  and  $\mathcal{S}^H$ . For visualisation purposes, values on the vertical axis correspond to a  $(r, \theta)$ -dependent linear combination  $P$  of  $p_r$  and  $p_\theta$ , such that  $P = p_r$  on  $\theta = 0.177$ . The section the invariant manifold cylinders on  $\theta = 0.177$ ,  $p_\theta > 0$  is highlighted. A representative trajectory is shown in cyan and the intersection with  $\theta = 0.177$ ,  $p_\theta > 0$  is marked with a cross. Configuration space projections of the periodic orbits and trajectory on a contour plot of the potential energy surface are added for illustration.

distinct mechanism of transport between the C-well and the H-well: a fast mechanism that takes trajectories from one well almost immediately to the other and a slow mechanism that leads trajectories via the flat region, the latter corresponding to roaming.

### Roaming

Each DS can be crossed by a trajectory in two directions, roughly speaking, in the direction of increasing or decreasing radius. These two halves are separated by the respective periodic orbits and will be referred to as inward and outward respectively. More details are in the Supporting information.

Roaming in the restricted acetaldehyde molecule is the transport of points from the outward half of  $\text{DS}_C$  to the inward half of  $\text{DS}_H$  via both halves of  $\text{DS}_f$ . This definition is consistent with the definition of roaming in formaldehyde [28].

Unstable periodic orbits have cylindrical stable and unstable invariant manifolds, that act as barriers to dynamics and mediate passage through the corresponding phase space bottleneck. The relevance of unstable periodic orbits was recognised by Pechukas and Pollak [31, 32] in the context of transition state theory. Dynamics in higher dimensional systems is governed by the manifolds of normally hyperbolic invariant manifolds [38, 39], of which an unstable periodic orbit is a 1-dimensional example.

A stable invariant manifold  $\mathcal{S}^\gamma$  of an unstable periodic orbit  $\gamma$  consist of trajectories that converge to  $\gamma$  as  $t \rightarrow \infty$ . Due to its cylindrical structure,  $\mathcal{S}^\gamma$  encloses a volume of trajectories that is conveyed to  $\text{DS}_\gamma$  at the narrowest part of the bottleneck. Trajectories not enclosed by  $\mathcal{S}^\gamma$  do not reach  $\text{DS}_\gamma$ . An unstable invariant manifold  $\mathcal{U}^\gamma$  consist of trajectories that converge to  $\gamma$  as  $t \rightarrow -\infty$ , but diverge in forward time.  $\mathcal{U}^\gamma$  encloses all trajectories that crossed  $\text{DS}_\gamma$  and guide them away. The roles of  $\mathcal{S}^\gamma$  and  $\mathcal{U}^\gamma$  reverse in backward time.

Each invariant manifold consists of two branches: one conveying trajectories to/from the inward half of  $\text{DS}_\gamma$  and one to/from the outward half. By definition a stable invariant manifold cannot intersect itself or another stable invariant manifold and the analogue is true for unstable invariant manifolds.

On the other hand, the intersection of  $\mathcal{U}^C$  and  $\mathcal{S}^H$  will guide trajectories from the outward half of  $\text{DS}_C$  to the inward half of  $\text{DS}_H$ , which is crucial for roaming. Radical dissociation is governed by the intersection of  $\mathcal{U}^C$  and  $\mathcal{S}^O$ .

The CH-orbit sets acetaldehyde apart from the likes of formaldehyde, Chesnavich's model or the double Morse. It allows  $\mathcal{U}^C$  and  $\mathcal{S}^H$  to intersect in two distinct regions:

- the region close to the wells near  $\text{DS}_C$  and  $\text{DS}_H$ ,

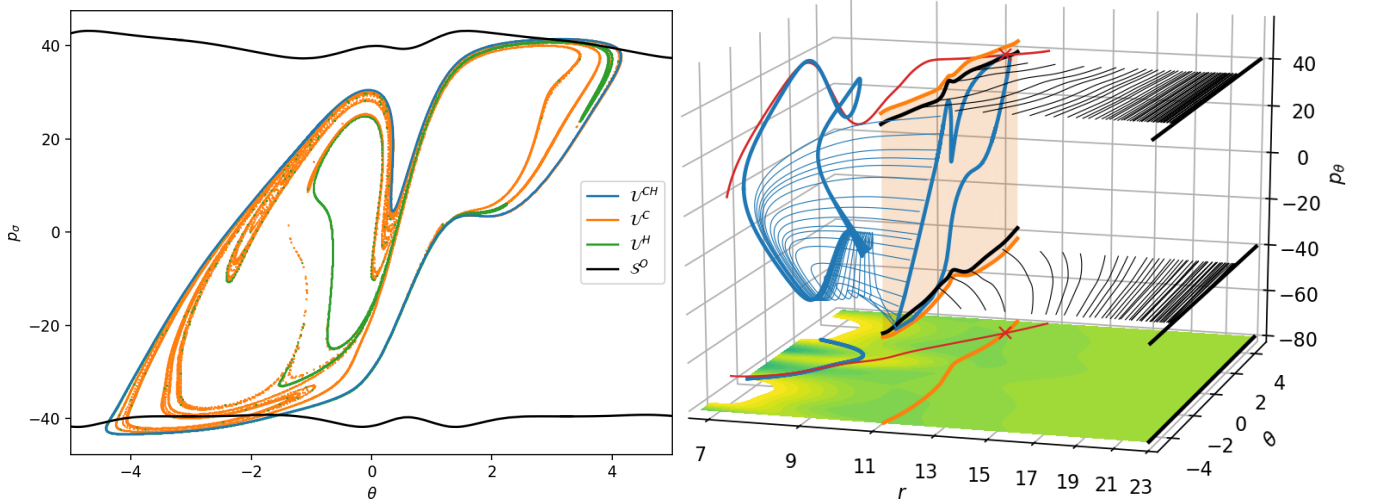


FIG. 6. The roaming mechanism conveying trajectories from the C-well to the H-Well via the flat region. Left: Intersection of  $U^{CH}$  and  $U^C$  with  $S^O$  on the outward annulus of  $DS_f$ . Right: A 3-dimensional projection of the intersection of  $U^{CH}$  and  $S^O$ . The section the invariant manifold cylinders on the outward annulus of  $DS_f$  is highlighted. A representative trajectory is shown in red and the intersection with the outward annulus of  $DS_f$  is marked with a cross. Configuration space projections of the periodic orbits and trajectory on a contour plot of the potential energy surface are added for illustration. Note that the  $r$ -axis is in log scale for better readability.

- the flat region beyond the CH-orbit,

separated by a phase space bottleneck associated with the CH-orbit. These two separate intersections form two different mechanisms for transport between the outward half of  $DS_C$  and the inward half of  $DS_H$ :

- a fast mechanism that takes trajectories from  $DS_C$  almost immediately to  $DS_H$ ,
- a slow mechanism that leads trajectories first to  $DS_f$  in the flat region - roaming.

Fig. 5 shows the intersection of  $U^C$  and  $S^H$  on the surface of section  $\theta = 0.177$ ,  $p_\theta > 0$ . These manifold intersections should be interpreted as reactive islands that do not form closed circles, because some trajectories on the manifolds are tangent to  $\theta = 0.177$ ,  $p_\theta > 0$ .  $U^{CH}$  and  $S^{CH}$  enclose the intersection of  $U^C$  and  $S^H$ , highlighting the fact that it does not pass through the phase space bottleneck associated with the CH-orbit. Only trajectories above  $S^{CH}$  and below  $U^{CH}$  pass through the bottleneck. A 3-dimensional representation of the mechanism is shown in Fig. 5.

Evidence for the slow, roaming mechanism, can be found in the flat region. As shown in the analysis of Chesnavich's  $CH_4^+$  system [23, 26], while the existence of a centrifugal barrier is necessary for roaming, the mechanism for roaming relies on the intersection of  $U^C$  and  $S^O$ . Fig. 6 shows the intersection of  $U^C$  and  $S^O$  on the outward annulus of  $DS_f$  and a 3-dimensional projection putting the intersection into wider mechanistic context.

The mechanism works in a simple way - all trajectories contained in the interior of both  $U^C$  and  $S^O$  dissociate immediately. Due to their intersection, there is a part of the interior of  $U^C$  that does not dissociate, but stays in the flat region. It exhibits chaotic behaviour due to the presence of pieces of stable and unstable invariant manifolds of all unstable periodic orbits that cause severe distortion.

The passage from the flat region to  $DS_H$  and the H-well is mediated by  $S^H$ . Due to time reversal symmetry,  $U^H$  and  $S^O$  intersect if and only if  $S^H$  and  $U^O$  intersect. The intersection of  $U^H$  and  $S^O$  is shown in Fig. 6.

We remark that a similar argument can be used to deduce the mechanism responsible for the passage from the flat region to  $DS_C$  and the C-well, that explains the two orange outliers in the histogram in Fig. 4.

The histogram in Fig. 4 further shows that roaming trajectories enter the H-well in 'packets' rather than being uniformly randomised. This agrees with a lobe dynamics [35] point of view, where trajectories contained in a lobe ('packet') share dynamical properties, such as in this case the number of rotations of  $CH_3$  around  $HCO$ . The peaks of the roaming time distribution are approximately 12616 time units apart, which corresponds to the period of the outer orbits. This also agrees with the existing classification of dynamical behaviour at constant kinetic energy [40].

## Discussion and conclusion

We found two mechanisms consisting of phase space structures that may lead to the same molecular products in a restricted acetaldehyde molecule. One of the mechanisms is a fast and direct passage between the C-well and the H-well, while the other is a slow passage via the flat region that fits the term frustrated dissociation and we refer to as roaming in this restricted molecule. This agrees with the findings of [27] that roaming is one of multiple channels leading to products with a particular energy distribution.

This work considers the dynamics at a single total energy, 0.01 a.u. above the dissociation threshold. At this energy we find the fast mechanism to dominate the roaming mechanism, both eclipsed by radical dissociation, similar to the proportions reported for formaldehyde [28].

Results on persistence of normally hyperbolic invariant manifolds under perturbations [38, 39] assure that all of the unstable periodic orbits involved in roaming persist for a range of energies around 0.01 a.u. As long as the periodic orbits creating the template for reaction mechanisms do not change, the reaction mechanisms themselves do not change qualitatively. Outside this energy range, bifurcations of periodic orbits are possible with resulting changes to reaction mechanism. The connection between bifurcations and changes in reaction mechanisms is the topic of ongoing research [26, 41].

Qualitatively we find that the roaming mechanisms of formaldehyde and restricted acetaldehyde bear remarkable similarities, the only differences induced by the CH-orbit and associated bottleneck. The CH-orbit in acetaldehyde is also responsible for the fast transport mechanism between the wells, which is absent in formaldehyde.

The existence of a bottleneck separating the wells from the flat region in acetaldehyde gives rise to a new reaction mechanism transporting trajectories between the wells. In the case of more complicated molecules, every additional bottleneck can be expected to give rise to at least one additional reaction mechanism. The necessary passage through multiple bottlenecks may decrease the proportion of roaming among competing mechanisms for molecular dissociation, but as long as the equivalents of  $\mathcal{U}^C$  and  $\mathcal{S}^O$  intersect, roaming will be present.

## Acknowledgments

We thank Prof. J. Bowman, Prof. Y.-C. Han and Prof. B. Fu for providing us with the potential energy surface of acetaldehyde. We acknowledge the support of EPSRC Grant no. EP/P021123/1 and Office of Naval Research (Grant No. N000141712220). We also acknowledge the high performance computing cluster Cream at the School of Mathematics and BlueCrystal at the Advanced Computing Research Centre of University of Bristol.

- 
- [1] R. D. van Zee, M. F. Foltz, and C. B. Moore, *J. Chem. Phys.* **99**, 1664 (1993).
  - [2] D. Townsend, S. A. Lahankar, S. K. Lee, S. D. Chambreau, A. G. Suits, X. Zhang, J. Rheinecker, L. Harding, and J. M. Bowman, *Science* **306**, 1158 (2004).
  - [3] S. A. Lahankar, S. D. Chambreau, D. Townsend, F. Suits, J. Farnum, X. Zhang, J. M. Bowman, and A. G. Suits, *The Journal of chemical physics* **125**, 044303 (2006).
  - [4] S. A. Lahankar, S. D. Chambreau, X. Zhang, J. M. Bowman, and A. G. Suits, *The Journal of chemical physics* **126**, 044314 (2007).
  - [5] S. Lahankar, V. Goncharov, F. Suits, J. Farnum, J. Bowman, and A. G. Suits, *Chemical Physics* **347**, 288 (2008).
  - [6] B. C. Shepler, Y. Han, and J. M. Bowman, *The Journal of Physical Chemistry Letters* **2**, 834 (2011).
  - [7] P. L. Houston, R. Conte, and J. M. Bowman, *The Journal of Physical Chemistry A* **120**, 5103 (2016).
  - [8] A. G. Suits, *Accounts of chemical research* **41**, 873 (2008).
  - [9] J. M. Bowman and A. G. Suits, *Physics today* **64**, 33 (2011).
  - [10] J. M. Bowman and B. C. Shepler, *Annual review of physical chemistry* **62**, 531 (2011).
  - [11] J. M. Bowman, *Molecular Physics* **112**, 2516 (2014).
  - [12] J. M. Bowman and P. L. Houston, *Chemical Society Reviews* **46**, 7615 (2017).
  - [13] F. A. Mauguière, P. Collins, Z. C. Kramer, B. K. Carpenter, G. S. Ezra, S. C. Farantos, and S. Wiggins, *Annual review of physical chemistry* **68**, 499 (2017).
  - [14] A. G. Suits, *Annual Review of Physical Chemistry* **71**, 77 (2020).
  - [15] F. A. Mauguière, P. Collins, G. S. Ezra, S. C. Farantos, and S. Wiggins, *Chemical Physics Letters* **592**, 282 (2014).
  - [16] P. Houston and S. Kable, *Proceedings of the National Academy of Sciences* **103**, 16079 (2006).
  - [17] B. C. Shepler, B. J. Braams, and J. M. Bowman, *The Journal of Physical Chemistry A* **112**, 9344 (2008).
  - [18] B. R. Heazlewood, M. J. Jordan, S. H. Kable, T. M. Selby, D. L. Osborn, B. C. Shepler, B. J. Braams, and J. M. Bowman, *Proceedings of the National Academy of Sciences* **105**, 12719 (2008).



- [19] K. L. K. Lee, M. S. Quinn, A. T. Maccarone, K. Nauta, P. L. Houston, S. A. Reid, M. J. Jordan, and S. H. Kable, *Chemical Science* **5**, 4633 (2014).
- [20] H.-K. Li, P.-Y. Tsai, K.-C. Hung, T. Kasai, and K.-C. Lin, *The Journal of Chemical Physics* **142**, 041101 (2015).
- [21] L. Rubio-Lago, G. Amaral, A. Arregui, J. Gonzalez-Vazquez, and L. Banares, *Physical Chemistry Chemical Physics* **14**, 6067 (2012).
- [22] L. Rubio-Lago, G. Amaral, A. Arregui, J. Izquierdo, F. Wang, D. Zaouris, T. Kitsopoulos, and L. Banares, *Physical Chemistry Chemical Physics* **9**, 6123 (2007).
- [23] V. Krajnák and S. Wiggins, *The Journal of chemical physics* **149**, 094109 (2018).
- [24] W. J. Chesnavich, *The Journal of chemical physics* **84**, 2615 (1986).
- [25] F. A. Mauguère, P. Collins, G. S. Ezra, S. C. Farantos, and S. Wiggins, *The Journal of chemical physics* **140**, 134112 (2014).
- [26] V. Krajnák and H. Waalkens, *Journal of mathematical chemistry* **56**, 2341 (2018).
- [27] C.-H. Yang, S. Bhattacharyya, L. Liu, W.-h. Fang, and K. Liu, *Chemical Science* , 6423 (2020).
- [28] F. A. Mauguère, P. Collins, Z. C. Kramer, B. K. Carpenter, G. S. Ezra, S. C. Farantos, and S. Wiggins, *The journal of physical chemistry letters* **6**, 4123 (2015).
- [29] Y.-C. Han, P.-Y. Tsai, J. M. Bowman, and K.-C. Lin, *Phys. Chem. Chem. Phys.* **19**, 18628 (2017).
- [30] F. G. Montoya and S. Wiggins, *Journal of Physics A: Mathematical and Theoretical* (2020), 10.1088/1751-8121/ab8b75.
- [31] E. Pollak and P. Pechukas, *J. Chem. Phys.* **69** (1978), 10.1063/1.436658.
- [32] P. Pechukas and E. Pollak, *J. Chem. Phys.* **71** (1979), 10.1063/1.438575.
- [33] P. Pechukas and E. Pollak, *The Journal of Chemical Physics* **71**, 2062 (1979).
- [34] H. Waalkens and S. Wiggins, *Journal of Physics A: Mathematical and Theoretical* **37**, L435 (2004).
- [35] V. Rom-Kedar and S. Wiggins, *Arch. Ration. Mech. Anal.* **109** (1990), 10.1007/BF00375090.
- [36] T. Uzer, C. Jaffé, J. Palacián, P. Yanguas, and S. Wiggins, *Nonlinearity* **15** (2002), 10.1088/0951-7715/15/4/301.
- [37] H. Waalkens and S. Wiggins, *J. Phys. A* **37** (2004), 10.1088/0305-4470/37/35/L02.
- [38] N. Fenichel, *Indiana Univ. Math. J* **21**, 1972 (1971).
- [39] S. Wiggins, *Normally hyperbolic invariant manifolds in dynamical systems* (Springer-Verlag, 1994).
- [40] V. Krajnák, G. S. Ezra, and S. Wiggins, *Regul. Chaotic Dyn.* **24**, 615 (2019).
- [41] V. Krajnák and H. Waalkens, *Journal of mathematical chemistry* **58**, 292339 (2020).
- [42] J. A. Jimnez Madrid and A. M. Mancho, *Chaos* **19**, 013111 (2009).
- [43] V. Krajnák, G. S. Ezra, and S. Wiggins, *International Journal of Bifurcation and Chaos* **30**, 2050076 (2020).
- [44] R. Bardakcioglu, A. Junginger, M. Feldmaier, J. Main, and R. Hernandez, *Phys. Rev. E* **98**, 032204 (2018).
- [45] F. A. L. Mauguère, P. Collins, Z. C. Kramer, B. K. Carpenter, G. S. Ezra, S. C. Farantos, and S. Wiggins, *J. Chem. Phys.* **144**, 054107 (2016).

## Supplementary information

### Equations of motion

The Hamiltonian

$$H(r, \theta, p_r, p_\theta) = \frac{p_r^2}{2\mu} + \frac{p_\theta^2}{2} \left( \frac{1}{I_{HCO}} + \frac{1}{\mu r^2} \right) + U(r, \theta), \quad (2)$$

defines the equations of motion

$$\begin{aligned} \dot{r} &= \frac{p_r}{\mu}, \\ \dot{p}_r &= \frac{p_\theta^2}{\mu r^3} - \frac{\partial U}{\partial r}, \\ \dot{\theta} &= p_\theta \left( \frac{1}{I_{HCO}} + \frac{1}{\mu r^2} \right), \\ \dot{p}_\theta &= -\frac{\partial U}{\partial \theta}. \end{aligned} \quad (3)$$

The value of the Hamiltonian is conserved along the solutions and therefore phase space is foliated by energy surfaces of the form  $H = E$ . Consequently surfaces such as  $\theta = 0.177$ ,  $p_\theta > 0$  and the outward part of  $DS_f$  used in this work are 2 dimensional at a fixed total energy.



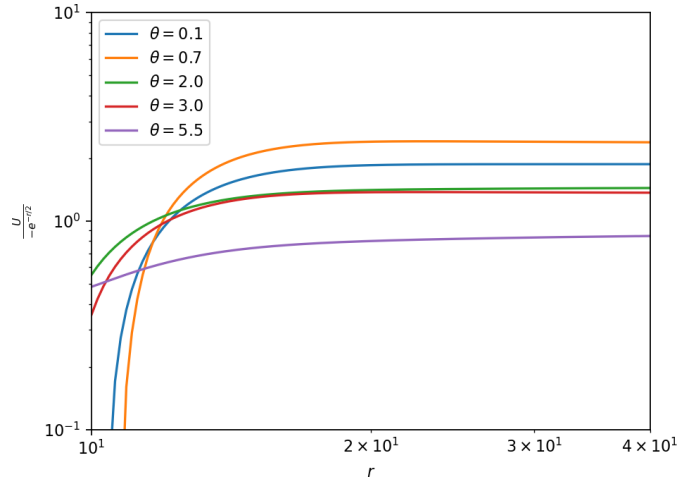


FIG. 7. Sections of  $\frac{U}{-e^{-r/2}}$  for constant values of the angle  $\theta$  showing that  $U \in O(e^{-r/2})$  as  $r \rightarrow \infty$ . A rate of convergence of the potential to the dissociation energy faster than  $r^{-2}$  assures the existence of a centrifugal barrier.

#### Finding periodic orbits

We find vibrational and rotational periodic orbits in different ways. Vibrational periodic orbits are characterised by two points at which kinetic energy vanishes and the all energy is in the potential component. These orbits can be found via bisection procedure along the equipotential line(s)  $U(r, \theta) = E$  initiated with  $p_r = p_\theta = 0$ .

Rotational periodic orbits require a different approach. Due to the absence of symmetries of this system, we used Lagrangian descriptors [42] in the sense as [43] to identify locations of nearly  $\theta$ -independent dynamics and subsequently employed the binary contraction method [44] to locate the outer and f-orbits.

Note that the existence of the outer periodic orbits is due to a centrifugal barrier that exists in any system for sufficiently low energies, provided the potential  $V$  approaches the dissociation energy at least  $V \in o(r^{-2})$  as  $r \rightarrow \infty$  [26]. In fact  $U$  converges faster,  $U \in O(e^{-r/2})$  as shown in Fig. 7.

#### Dividing surfaces

Dividing surfaces (DS) are constructed using periodic orbits as follows. We remark that while the instability of a periodic orbit assures locally minimal flux across the DS, the construction can be done using any periodic orbit.

Let  $\Gamma$  be a periodic orbit. For any point  $(r_\Gamma, \theta_\Gamma)$  on the configuration space projection of  $\Gamma$ , consider all values of  $p_r$  and  $p_\theta$ , such that the point  $(r_\Gamma, p_r, \theta_\Gamma, p_\theta)$  lies on the energy surface. All such points project onto  $(r_\Gamma, \theta_\Gamma)$  and satisfy

$$\frac{p_r^2}{2\mu} + \frac{p_\theta^2}{2} \left( \frac{1}{I_{HCO}} + \frac{1}{\mu r_\Gamma^2} \right) = H - U(r_\Gamma, \theta_\Gamma).$$

On the energy surface this set is a circle and collapses to a point if  $H = U(r_\Gamma, \theta_\Gamma)$ . We define the DS as the union of these sets over all points  $(r_\Gamma, \theta_\Gamma)$ .

As  $H = U(r, \theta)$  at the turning points of the corresponding orbits, both  $DS_C$  and  $DS_H$  are spheres consisting of a continuum of circles and two points at the poles. The construction above is known to provide a DS that is transversal to the Hamiltonian vector field, in our case (3), except at the periodic orbit [33, 34].

The construction of a DS is identical for a pair of rotational periodic orbits, such as the f-orbits or the outer orbits, since the orbits share a configuration space projection and only differ in the sign of their momenta. Since  $H > U(r, \theta)$  along rotational periodic orbits, the DS is known to be a torus and transversal to the Hamiltonian vector field [45].

Note that DSs are not unique, as any deformation of the above-constructed DS that does not violate transversality to the vector field is also a DS.

Each of the above-defined DSs can be split in two halves: spheres are split into two hemispheres bounded by their respective periodic orbit, tori into two annuli bounded by their two orbits. Due to transversality, each half must be crossed by trajectories in the same direction, for example in the case of  $DS_C$  escape from the bound states of

acetaldehyde. Due to conservation of volume, the flux across the two halves must be equal in magnitude and opposite in direction.

In literature, the hemisphere of  $DS_C$  through which trajectories escape from the bound states of acetaldehyde would be referred to as the outward hemisphere. Similarly the inward hemisphere is the one through which trajectories enter the bound states of acetaldehyde.

#### *Invariant manifolds*

Stable and unstable invariant manifolds of unstable periodic orbits are calculated using a monodromy matrix as detailed in [41].